Self-Healing Properties of Poly(Ethylene-*co*-Vinyl Acetate)

Ryuya Osato,[1)] Takumi Sako,[1)] Jiraporn Seemork,[1),2)] Sunatda Arayachukiat,[1)] Shogo Nobukawa,[1)] Masayuki Yamaguchi[1)]*

1) School of Materials Science, Japan Advanced Institute of Science and Technology, 1-1 Asahidai, Nomi, Ishikawa 923-1292, Japan
2) Program in Petrochemistry, Faculty of Science, Chulalongkorn University, Pathumwan, Bangkok 10330, Thailand

* Corresponding author:
E-mail; m_yama@jaist.ac.jp
TEL +81-761-51-1621; FAX +81-761-51-1149

Abstract

Poly(ethylene-*co*-vinyl acetate) with 42 wt.% of vinyl acetate shows autonomic self-healing at room temperature without macroscopic flow. Intermolecular diffusion of amorphous chains through the jointed boundary, which occurs because of the large amount of amorphous chains with low glass transition temperature, is responsible for the healing phenomenon. Furthermore, the healing efficiency is found to be enhanced when the separated pieces are recombined immediately after cutting. This result indicates that the cut surface has marked molecular mobility owing to the destruction of crystallites during the cutting process, which is supported by differential scanning calorimetry measurements. The marked molecular mobility at the surface is, however, observed only for a short period after cutting, because further crystallization after cutting restricts the molecular motion.

Keywords; ethylene-*co*-vinyl acetate copolymer; self-healing; rheology; crystallinity

Introduction

Various approaches have been used to develop a self-healing polymer, one of the proposed smart materials, to effectively expand the lifetime of polymer products [1-8]. The healing methods reported in the literature may be roughly classified into four groups; (1) reversible chemical reactions such as Diels-Alder/Retro Diels-Alder, (2) composites containing microcapsules or hollow-fibers in which a healing agent is loaded, (3) intermolecular interactions between specific groups such as hydrogen bonding, ionic interaction, and π–π stacking interaction, and (4) molecular interdiffusion.

In the cases of methods (1)–(3), most studies have been performed using elastomers and thermosetting resins. This is reasonable because during repair random recombination between neighbor molecules will provide a network structure. From the viewpoint of industrial applications, however, poor cost-performance is a great problem for these methods. Furthermore, each of these methods has restricted application because of the complicated chemical structures of the molecules involved, which is another serious problem for the commercialization.

In contrast, for amorphous polymers, intermolecular interdiffusion occurs beyond the glass transition temperature T_g, and they can be used for healing without further chemical modification. However, to the best of our knowledge, this method has not yet been used in industry because precise temperature control is required for healing without macroscopic flow. Meanwhile, our research group has previously reported that weak gels having many dangling chains show autonomic healing without the involvement of any manual operations or chemical reactions [7,9,10]. The dangling chains, the molecular weight of which must be higher than the entanglement molecular

weight, are responsible for the healing behavior via intermolecular diffusion, while the network structure of the gel prohibits macroscopic flow. Up to now, a weak gel of polyurethane was developed, which shows the excellent healing behavior [9]. Moreover, a precise control of the glass transition temperature made it possible to develop a self-healing polymer with a relatively high modulus at room temperature, e.g, 100 MPa, which was composed of polyurethane and cellulose esters [7]. Although precise temperature control to repair is not needed for this material, it has not been used in industry because of its thermosetting nature. In this paper, we have further investigated this concept, i.e., a weak gel method, using a crystalline polymer with a low degree of crystallinity. Because the crystalline phase can act as a source of crosslinking points below the melting point, the mechanical behavior including molecular motion must be similar to that of a weak gel with chemical crosslinking points. Furthermore, various thermoplastic processing operations must be available for a crystalline polymer beyond its melting point, which is significantly different from the self-healing network polymers developed.

At present, various crystalline polymers with a low degree of crystallinity are commercially available, such as poly(vinyl chloride) (PVC) [11,12], cellulose esters [13], quenched poly(ethylene-terephthalate) and/or its copolymers [14-16], and poly(lactic acid) [17,18]. In this study, poly(ethylene-*co*-vinyl acetate) (EVA) is employed as a polymer with a low degree of crystallinity to evaluate the self-healing ability at room temperature, because its T_g is lower than room temperature. This suggests that autonomic healing by molecular motion may be expected even at room temperature. Such a study, to the best of our knowledge, has not been reported yet.

Since EVA is a commercially available with good cost-performance, the impact of the research on the industry must be significant.

Experimental

Materials

The material used was a commercially available EVA with 42 wt.% of vinyl acetate. The number- and weight-average molecular weights, evaluated by size exclusion chromatography (HLC-8121GPC/HT, Tosoh, Japan) of TSK_{gel} GMH_{HR}-H(20)HT and TSK_{gel} GMH_6-HTL with 1, 2, 4-trichlorobenzene at 140 °C as an eluent, were 8.0×10^3 and 2.7×10^4, respectively, as a linear polyethylene standard.

The pellet form sample was compressed into a flat sheet with 3 mm thickness using a compression-molding machine at 150 °C for 3 min. The obtained sheet was subsequently cooled at 5 °C for 3 min using another compression-molding machine. After processing, the samples were immediately used for measurements. In the case of the evaluation of self-healing ability, the samples were kept at 25 °C for 10 min or 64 h prior to cutting, as explained in detail later.

Measurements

Melting characteristics were evaluated using a differential scanning calorimeter (DSC820, Mettler-Toredo, USA) under nitrogen atmosphere. Approximately 10 mg of the sample was put into an aluminum pan. After cooling to −20 °C, the sample was heated at a rate of 10 °C/min to evaluate its melting point and enthalpy of fusion. The degree of crystallinity X_c (%) was calculated by the enthalpy of fusion $\Delta H_{measured}$ measured during the first scan;

$$X_c = \frac{\Delta H_{measured}}{\Delta H_{perfect}} \times 100 \quad (1)$$

where $\Delta H_{perfect}$ is the enthalpy of fusion of the perfect crystal.

Wide-angle X-ray diffraction (WAXD) patterns were obtained using a graphite-monochromatized CuKα radiation beam focused via a 0.3-mm pinhole collimator with a flat 20 × 20 cm^2 imaging plate (IP) detector of 1900 × 1900 pixels (R-AXIS IIc, Rigaku, Japan). The exposure was performed with 7 min per shot by directing the X-ray beam in the normal direction of the plate.

The temperature dependence of the oscillatory tensile modulus of the samples was measured at 10 Hz using a dynamic mechanical analyzer (Rheogel E4000-DVE, UBM, Japan) at a heating rate of 2 °C/min. Samples 2 mm in width and 10 mm in length were cut from the sheet for the measurements.

The self-healing properties of the samples were evaluated using a uniaxial tensile machine (LSC-50/300, Tokyo Testing Machine, Japan) at 25 °C. The crosshead speed was 10 mm/min and the initial gauge length was 10 mm. The sample preparation procedure is shown in Fig. 1.

[Fig. 1]

After the compression-molding, the samples were cut into rectangular shapes of 10 mm in width and 30 mm in length and kept in a temperature-humidity controlled chamber (IG420, Yamato, Japan) at 25 °C and 50 % relative humidity for 10 min ((A) and (C) in Fig. 1) or 64 h ((B) and (D)). After removal of the samples from the chamber, they were cut into two pieces using a razor blade. Then, to begin the recombination process, the cut surfaces of the pieces were reattached by manual operation with slight pressure to avoid the formation of air bubbles between the surfaces. After joining, the

pressure was removed. The recombination process was performed immediately after cutting ((A) and (B)) or after leaving the cut pieces in the controlled chamber at 25 ºC for 3 (C) or 64 hours ((C) and (D)). The recombined samples were then kept in the temperature-humidity controlled chamber at 25 °C for 64 h prior to the tensile test. In the case of (A), the samples were kept in the chamber for various periods to evaluate the effect of the attached period on the healing behavior. All tensile tests were performed at least 10 times and the average value was calculated.

Results and Discussion

Characteristics of the sample

Commercially available EVA is known to be a crystalline polymer. Therefore, it can be provided in pellet form, as was the sample used in this study, even though its T_g is lower than room temperature. According to previous studies [19-24], EVA shows crystallinity originating from the ethylene sequence when the vinyl acetate content is lower than 50 wt.%. Therefore, the crystallinity and melting point of EVA decrease with increasing vinyl acetate content.

Because the sample used in this study contained 42 wt.% of vinyl acetate, it exhibited crystallinity. The melting point T_m and the enthalpy of fusion of the sample were determined from the obtained DSC heating curves. Prior to measurements, the samples were encapsulated in an aluminum pan immediately after the compression-molding, and then kept at 25 °C for various periods. It was found that the melting characteristics of the samples were affected by the time after the compression-molding, as shown in Fig. 2. The effect was prominent within a relatively short period (< one day). This phenomenon is observed for most crystalline polymers

with low T_g [25,26], because molecular motion is allowed to some degree in such polymers even at room temperature. The crystallinity of the present sample was calculated to be around 3 %, assuming that the enthalpy of fusion of perfectly crystalline polyethylene is 293 J/g [27]. This degree of crystallinity is almost identical to that reported previously [19-24]. Moreover, the enthalpy of fusion was found to become almost constant one day after the compression-molding. To characterize the crystalline phase, the wide-angle X-ray diffraction pattern of the sample was measured. However, owing to the low degree of crystallinity, only a broad amorphous peak was detected (not presented).

[Fig. 2]

Fig. 3 shows the temperature dependence of the tensile storage modulus *E'* and loss modulus *E"* at 10 Hz of the sample. The sample for the measurement was used immediately after the compression-molding. As seen in the figure, T_g, defined as the peak temperature in the *E"* curve, was around −30 °C, which corresponds with the previously reported value [19,21]. Beyond T_g, both moduli decreased gradually with temperature and fell off sharply at 40 °C, which is attributed to the melting of crystals. At room temperature, therefore, the storage modulus was almost the same as that of a typical rubber [28]. In other words, a flexible network structure formed at room temperature via the physical crosslinking points of the crystals. In fact, the sample never flowed macroscopically at room temperature.

[Fig. 3]

Self-healing behavior

Fig. 4 shows the stress-strain curves for recombined samples, i.e., healed samples, with different healing periods at 25 °C. The given stress and strain are the engineering values. The samples were cut immediately after the compression-molding, i.e., method (A) in Fig. 1. In the figure, the stress-strain curve for the virgin sample, i.e., an uncut sample, is also shown as a reference. Although the initial part of the stress-strain curves for all recombined samples was the same as that for the virgin sample, the strain at break was sensitive to the length of the healing period prior to the tensile measurement. As seen in the figure, the sample with a short healing period showed an immediate break after stretching. In contrast, the samples with a prolonged healing could be elongated to some degree. This result indicates that the adhesive strength increased with healing period length. Furthermore, the Young's modulus was repaired to the original value.

[Fig. 4]

The behavior of the sample specimens during the tensile tests are exemplified in Fig. 5. Both samples were prepared following method (A) in Fig. 1, with different healing periods prior to the tensile test. The sample with a prolonged healing period could be elongated with a tensile strain of 1.0.

[Fig. 5]

The observed healing behavior may have originated from the interdiffusion of amorphous chains through the joined boundary. The mechanism was well summarized by Wool [1], although the present system contained crystallites. Moreover, the enhanced adhesion attributed to the crystal growth at the attached surfaces may also be a possible mechanism for the repair, because the present samples were cooled in a short time, i.e.,

3 min at 5 °C, during the compression-molding. Therefore, the crystals were not developed enough as demonstrated in Fig. 2.

Comparing methods (A) and (B), crystal growth prior to cutting did not greatly affect the healing behavior of the samples as shown in Fig. 6. However, when the cut pieces were not recombined together immediately, i.e., methods (C) and (D), the healing efficiency decreased greatly even with the same healing period (64 h) after the recombination. These results suggest that the degree of crystallinity at the cut surface was initially low, and eventually increased with time. Because of the low crystallinity after cutting, the interdiffusion of amorphous chains through the boundary would be pronounced. After 64 h, however, the crystal growth at the surface reduced the molecular mobility, leading to poor healing.

[Fig. 6]

Information on the surface crystallinity was easily obtained by DSC measurements. For this experiment, the sample for measurement was cut into small pieces to increase its surface area. The details of the sample preparation are illustrated in the supplementary information. The dimensions of the large piece employed in procedure (a) were approximately 3 × 3 × 1.1 (mm), whereas those of the small pieces prepared by procedures (b) and (c) were around 0.7 × 0.7 × 0.7 (mm^3). Therefore, the surface area of the large piece was approximately 3 mm^2. In the case of the samples prepared by procedures (b) and (c), 30 small pieces were encapsulated in one aluminum pan for the measurement. Consequently, the total surface area of the small pieces was almost 3 times as large as that of the large piece, while the total volume/weight was similar.

As seen in Fig. 7, the DSC heating curve of the sample prepared by procedure (c) was almost the same as that of the original one 64 h after cutting (procedure (a)), suggesting that the crystallinity before cutting did not have a serious impact on the crystallinity observed after 64 h, including that of the surface. In contrast, the enthalpy of fusion in the low temperature region was pronounced and the main peak was reduced for the sample prepared by procedure (b) compared with those of the others. The melting point depression suggests that the surface area of crystals was enhanced [29]. In other words, crystals in the virgin sample were fragmented into small pieces by the applied force during the cutting process, which has been reported for other crystalline polymers [30]. This fragmentation of crystals was responsible for the marked chain mobility and thus the healing behavior. After the cut surface was left exposed for a while, however, the chain mobility was suppressed by further crystallization, leading to poor healing. The schematic illustration of this mechanism is shown in the supplementary information.

[Fig. 7]

The effect of the holding time after cutting on the healing behavior was also evaluated. The samples were cut immediately (10 min) after the compression-molding, i.e., method (C) in Fig. 1. As shown in Fig. 8, the samples recombined at 3 or 64 h after cutting exhibited poor healing, i.e., small strains at break, compared with that recombined immediately (“0 h”, which corresponds to the method (A) with 64 h of the healing). The degree of crystallinity, i.e., heat of fusion, showed a similar tendency as that observed for the strain at break. This result also demonstrates that the decrease in surface crystallinity caused by the cutting was responsible for the marked healing.

[Fig. 8]

For improved healing ability based on the present experimental results, additional techniques will be required in future for practical application because immediate attachment after cutting is required. However, the results obtained in this study provide a principle upon which the self-healing behavior of a crystalline polymer with low crystallinity may be enhanced.

Conclusion

The self-healing properties of a low crystallinity polymer with low T_g was studied using poly(ethylene-*co*-vinyl acetate) with 42 wt.% of vinyl acetate. The samples were cut into two pieces and recombined. The samples exhibited autonomic self-healing at room temperature which increased with the length of the healing period. The observed healing behavior is attributed to the intermolecular diffusion of amorphous chains. Furthermore, the healing behavior was enhanced when the separated pieces were joined together immediately after the cutting process because crystallites in the samples were destroyed by the cutting to some degree. In other words, an increase in the amount of amorphous chains was responsible for the marked mobility at the cut surface. However, the molecular mobility, and thus the self-healing behavior, was eventually reduced by further crystallization at the surface. The healing behavior observed in this study is expected for all crystalline polymers with a low degree of crystallinity when the T_g of the material is lower than the ambient temperature.

Acknowledgement

This work was promoted by COI program “Construction of next-generation infrastructure system using innovative materials” – Realization of safe and secure

society that can coexist with the Earth for centuries – Supported by Japan Science and Technology Agency (JST). Further, a part of this study was supported by Grand-in-Aid for Scientific Research No.25410221.

Reference

1. Wool RP, Polymer interfaces: Structure and strength, Hanser Gardener, Cincinnati, 1994.
2. Wool RP (2008) Self-healing materials; a review. Soft Matter 4:400-418.
3. Wu DY, Meure S, Solomon D (2008) Self-healing polymeric materials; A review of recent developments. Prog Polym Sci 33:479-522.
4. Blaszik BJ, Kramer SLB, Olugebefola SC, Moore JS, Sottos NR, White SR (2010) Self-healing polymers and composites. Annu Rev Mater Res 40:179-211.
5. Murphy B, Wudl F (2010) The world of smart healable materials. Prog Polym Sci 35:223-251.
6. Zhang MQ, Rong MZ, Self-healing polymers and polymer composites, Wiley, New York, 2010.
7. Yamaguchi M, Maeda R, Kobayashi R, Wada T, Ono S, Nobukawa S (2012) Autonomic healing and welding by interdiffusion of dangling chains in weak gel. Polym Intern 61:9-16.
8. Binder WH, Self-healing polymers, from principles to applications, Wiley-VCH, Weinheim, 2013.
9. Yamaguchi M, Ono S, Terano M (2007) Self-repairing property of polymer network with dangling chains. Mater Lett 61:1396-1399.
10. Yamaguchi M, Ono S, Okamoto K (2009) Interdiffusion of dangling chains in weak gel and its application to self-repairing material. Mater Sci Eng B 162:189-194.
11. Summers JW (1981) The nature of poly(vinyl chloride) crystallinity – the microdomain structure. J Vinyl Technol 3:107-110.
12. Yamaguchi M (2001) Flow instability in capillary extrusion of plasticized poly(vinyl chloride). J Appl Polym Sci 82:1277-1283.
13. Nobukawa S, Shimada H, Aoki Y, Miyagawa A, Doan VA, Yoshimura H, Tachikawa Y, Yamaguchi M (2014) Extraordinary wavelength dispersion of birefringence in cellulose triacetate film with anisotropic nanopores. Polymer 55:3247-3253.
14. Yamaguchi M, Wakabayashi T (2006) Rheological properties and processability of chemically modified poly(ethylene terephthalate-co-ethylene isophthalate). Adv Polym Technol 25:236-241.

15. Yamaguchi M, Wakabayashi T, Kanoh T (2008) Effect of mixing conditions on rheological and optical properties for chemically modified poly(ethylene terephthalate-co-ethylene isophthalate). J Appl Polym Sci 107:2665-2670.
16. Rujirek W, Hachiya Y, Endo T, Nobukawa S, Yamaguchi M (2015) Anomalous transfer phenomenon of carbon nanotube in the blend of poly(ethylene terephthalate) and polycarbonate. Composites Part B 78:409-414.
17. Yamane H, Sakai K, Takano M, Takahashi M (2004) Poly(D-lactic acid) as a rheological modifier of poly(L-lactic acid): Shear and biaxial extensional flow behavior. J Rheol 48:599-609.
18. Jimenez A, Peltzer M, Ruseckaite R, Poly(lactic acid) Science and Technology: Processing, Properties, Additives, and Applications, Royal Society of Chemistry, Oxfordshire, 2014.
19. Salyer IO, Kenyon AS (1971) Structure and property relationships of ethylene-vinyl acetate copolymers. J Polym Sci Part A-1 9:3083-3103.
20. Shankernarayanan MJ, Sun DC, Kojima M, Magill JH (1987) Rolletrusion: Doubly-orientation processing and morphology – Property relationships for commercial plastics. Intern Polym Proc 1:66-76.
21. Arsac A, Carrot C, Guillet J (1999) Rheological characterization of ethylene vinyl acetate copolymer. J Appl Polym Sci 74:2625-2630.
22. Dlubek G, Lpke Th, Stejny J, Alam MA, Arnold M (2000) Local free volume in ethylene-vinyl acetate copolymers: A positron lifetime study. Macromolecules 33:990-996.
23. Peacock AJ, Handbook of Polyethylene, Marcel Dekker, New York, 2000
24. Takahashi S, Okada H, Nobukawa S, Yamaguchi M (2012) Optical properties of polymer blends composed of poly(methyl methacrylate) and ethylene-vinyl acetate copolymer. Eur Polym J 48:974-980.
25. Yamaguchi M, Arakawa K (2007) Control of structure and mechanical properties for binary blends of poly(3-hydroxybutyrate) and cellulose-derivative. J Appl Polym Sci 103:3447-3452.
26. Huang T, Miura M, Nobukawa S, Yamaguchi M (2014) Crystallization behavior and dynamic mechanical properties of poly(L-lactic acid) with poly(ethylene glycol) terminated by benzoate. J Polym Environment 22:183-189.
27. Zhu L, Polymer Handbook 4th Edition, Eds. J. Brandrup, E.H. Immergut, E.A. Grulke, V/9-19, Wiley Interscience, New York, 1999.
28. Ferry JD, Viscoelastic properties of polymers, 3rd Ed., Wiley, New York, 1980.
29. Wunderlich B, Macromolecular Physics, Vol. 3, Crystal Melting, Academic Press, New York, 1980.
30. Rodriguez-Cabello JC, Alonso M, Merino JC, Pasor JM (1996) Scanning electron microscopy and differential scanning calorimetry study of the transition front in uniaxially stretched isotactic polypropylene. J Appl Polym Sci 60:1709-1717.

Figure Captions

Figure 1 Schematic illustration of the sample preparation methods for the tensile test. All procedures were carried out at 25 °C. The dimensions of the initial sample shape before cutting were 10 mm width, 30 mm length, and 3 mm thickness. After keeping the samples in the temperature-humidity controlled chamber for 10 min or 64 h, they were cut into two pieces with a razor blade. The cut pieces were reattached with slight pressure immediately after cutting ((A) and (B)) or after leaving the pieces for 3 (C) or 64 h ((C) and (D)). The healing was performed for 64 h except for (A).

Figure 2 Growth curves of the melting point T_m and the heat of fusion after the compression-molding.

Figure 3 Temperature dependence of (closed) tensile storage modulus *E'* and (open) loss modulus *E"* at 10 Hz.

Figure 4 Stress-strain curves of samples with different healing periods from 1 min (0.017) to 336 h, denoted by the numerals (h). The samples were prepared by method (A) in Fig. 1. In the figure, the curve of the original sample (virgin) without cutting is also shown.

Figure 5 Pictures during the tensile test for healed samples with different healing periods at 25 °C; (top) 1 min and (bottom) 64 h. The numerals below the pictures represent the tensile strain.

Figure 6 Strain at break evaluated by tensile tests for the samples prepared by methods (A), (B), (C) and (D) in Fig. 1. In the case of (A), the recombined pieces were healed for 64 h, and the cut pieces were recombined for 64 h after cutting for (C).

Figure 7 DSC heating curves measured at a rate of 10 °C/min for the samples obtained by procedures (a), (b), and (c) in Fig. 7.

Figure 8 Strain at break (open bars) for samples with different holding times at 25 °C before recombination; the samples left for 3 and 64 h were prepared by method (C) in Fig. 1. The sample with 0 h was prepared by method (A) with a 64 h healing period.

The filled bars represent the heat of fusion for the corresponding samples; 30 small pieces of 0.7 × 0.7 × 0.7 mm^3 in size were cut from the sheet 10 min after the compression-molding and left for 0, 3, and 64 h at 25 °C prior to the DSC measurements.

Supplementary information 1

Schematic illustration of the sample preparation procedures for the DSC surface crystallinity evaluation measurements: (a) a large piece measuring 3 × 3 × 1.1 mm^3 was cut out from the compressed sheet and kept at 25 °C for 64 h prior to the measurement, (b) 30 small pieces each with dimensions of 0.7 × 0.7 × 0.7 mm^3 were cut from the compressed sheet and used immediately after cutting, and (c) the small pieces were kept at 25 °C for 64 h prior to the measurement.

Supplementary information 2

Schematic illustration of molecular chains after cutting.

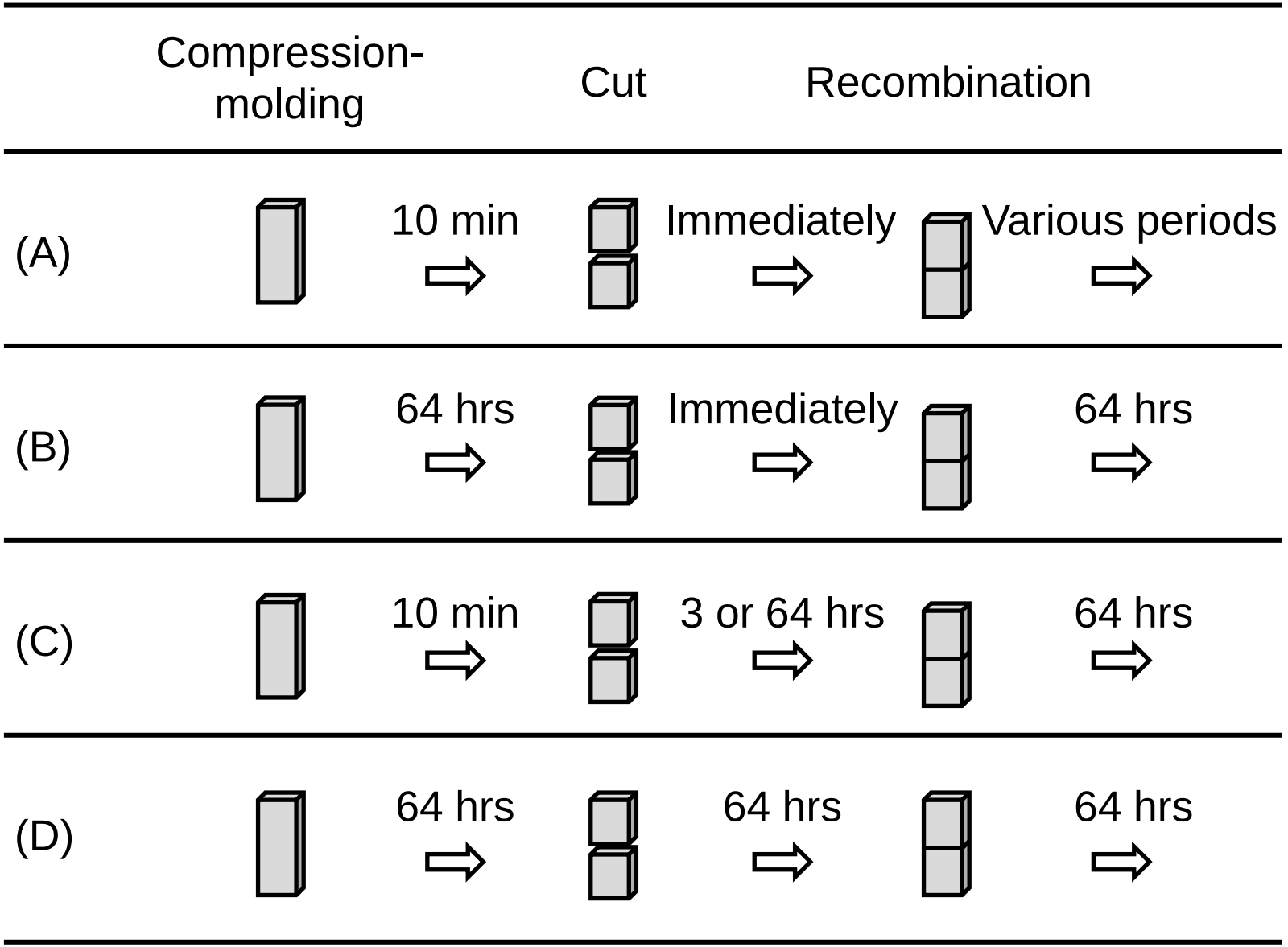

Osato et al., Figure 1

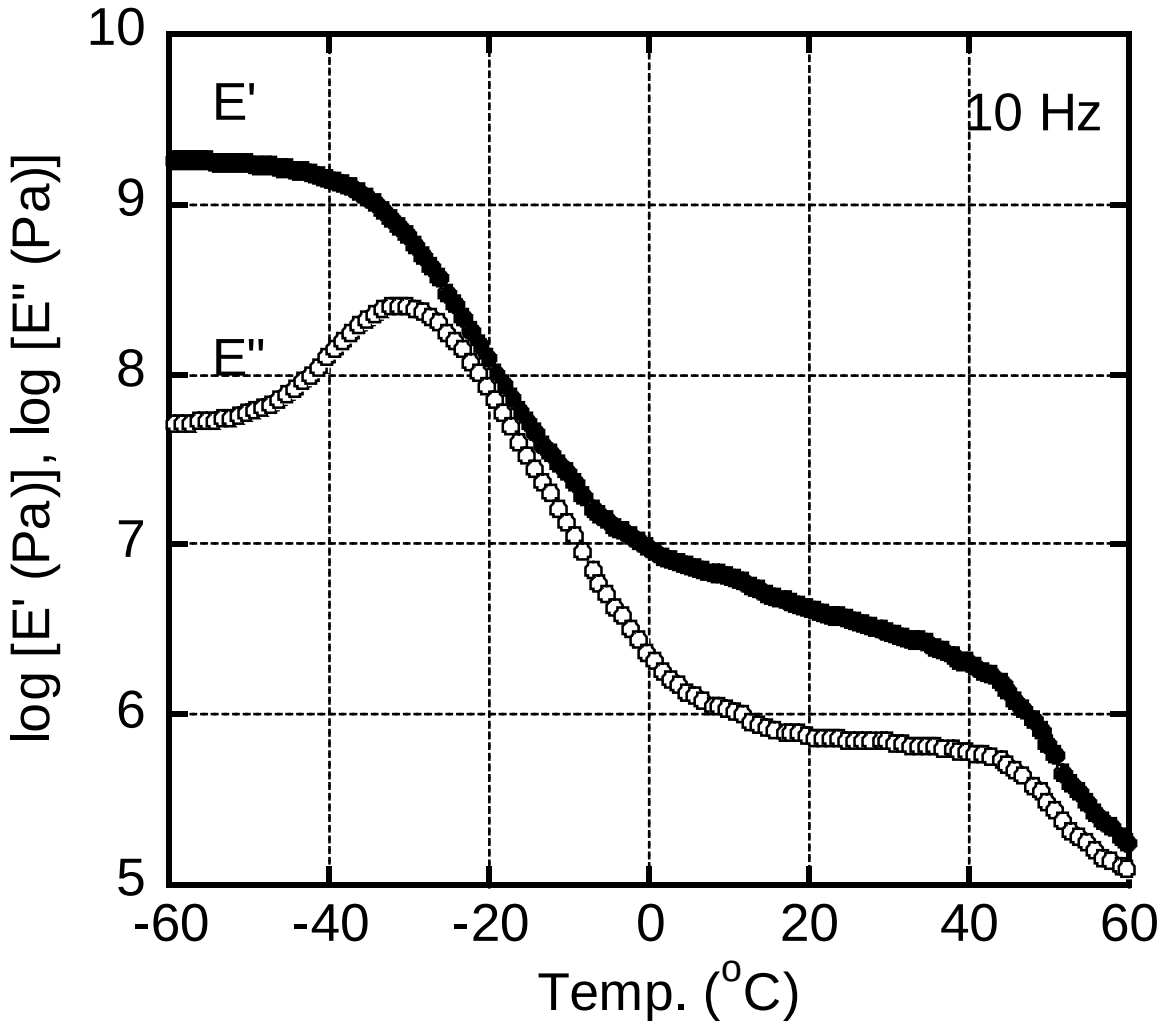

Osato et al., Figure 2

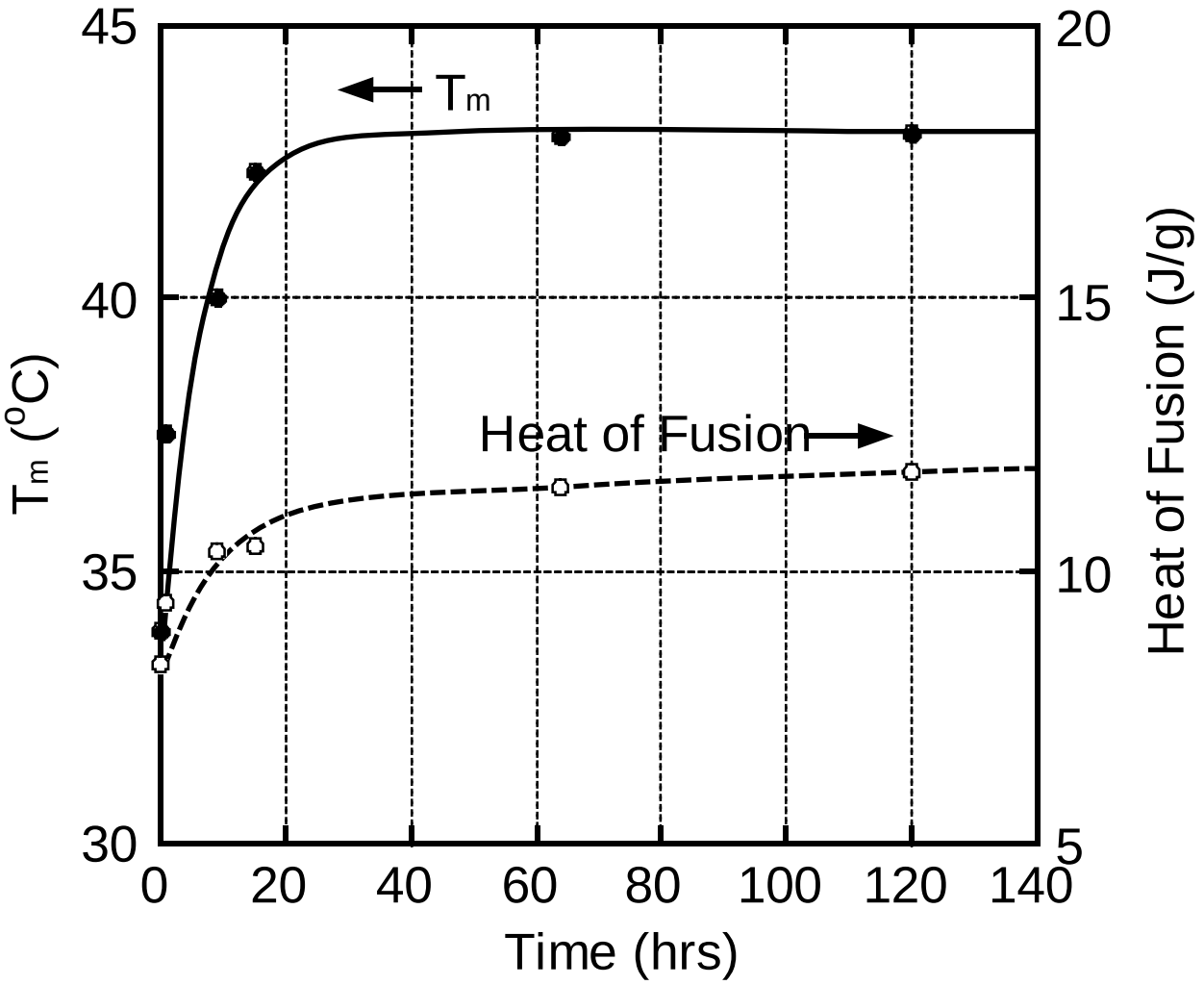

Osato et al., Figure 3

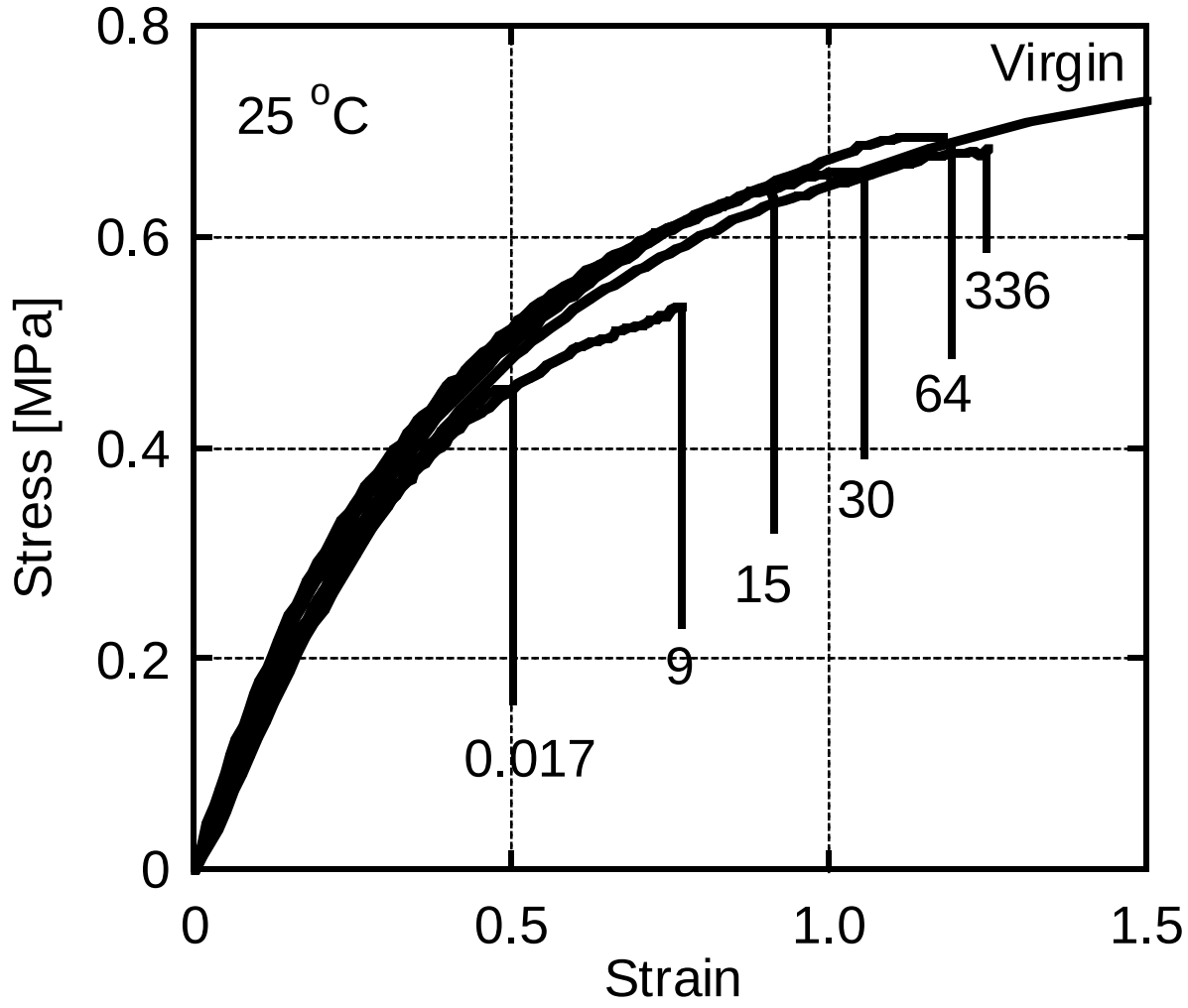

Osato et al., Figure 4

1 min after recombination

Strain : 0

0.5

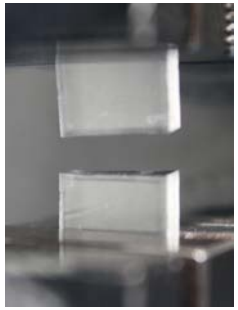

0.6

64 hrs after recombination

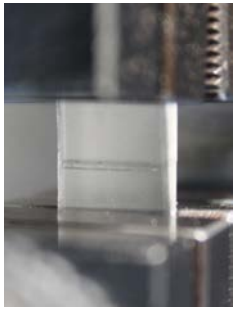

Strain : 0

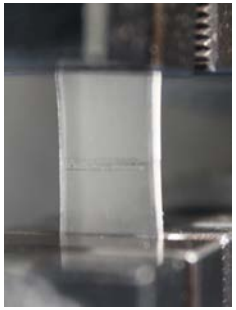

0.5

1.0

Osato et al., Figure 5

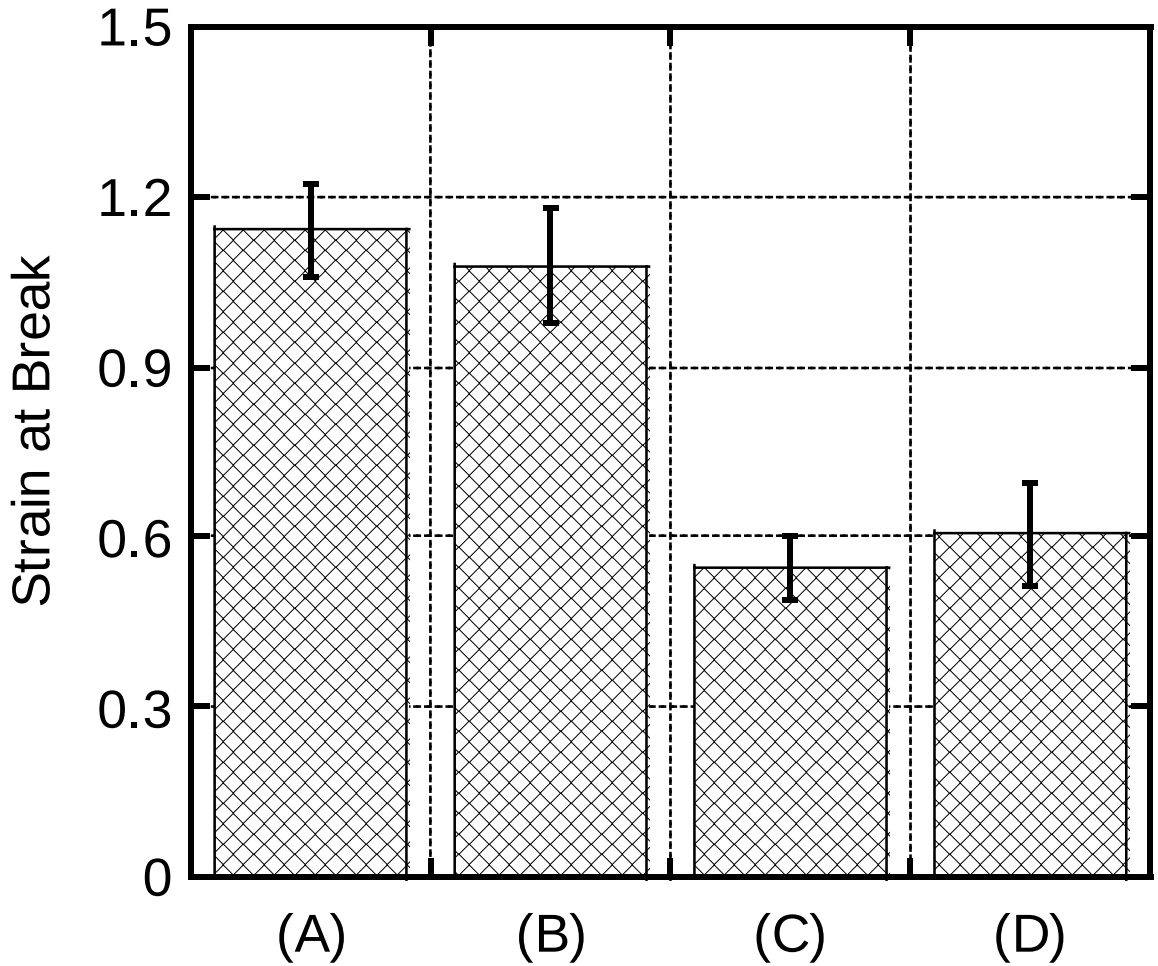

Osato et al., Figure 6

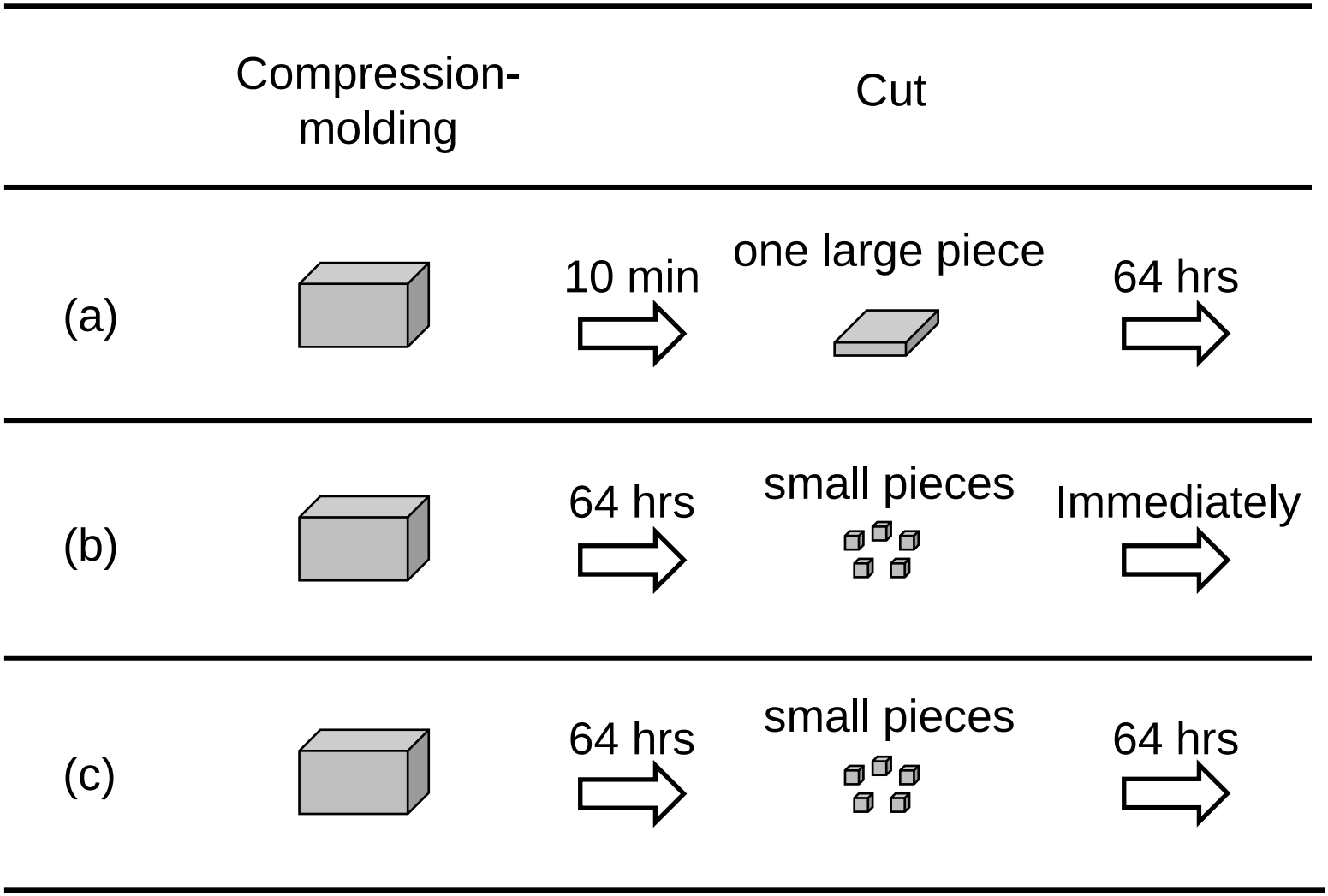

Osato et al., Figure 7

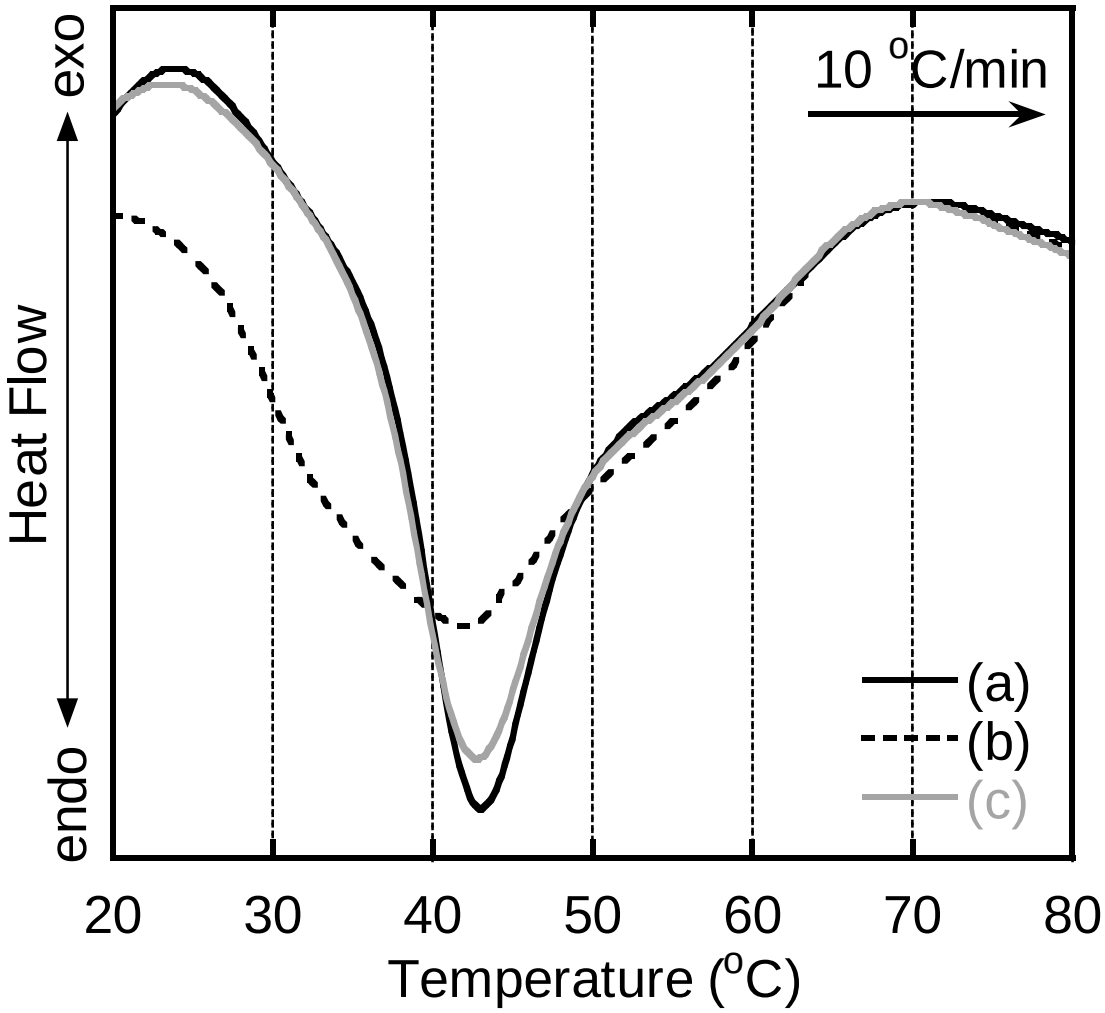

Osato et al., Figure 8

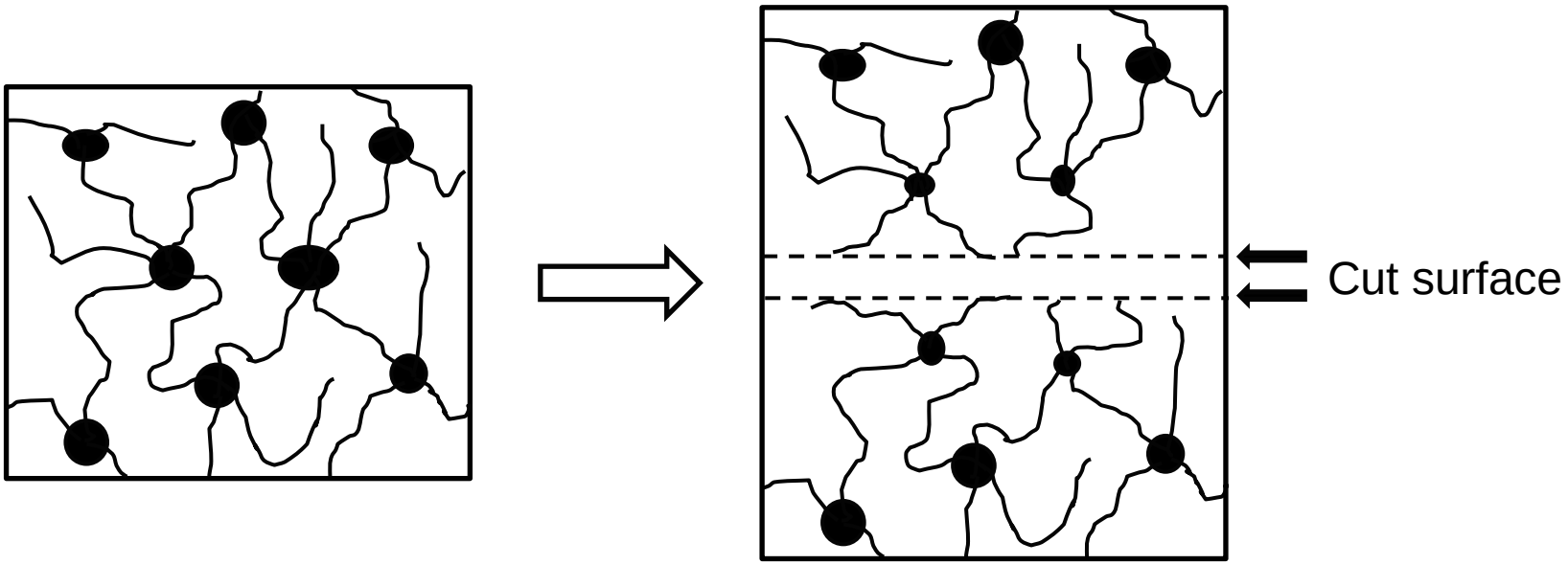

Osato et al., Figure 9

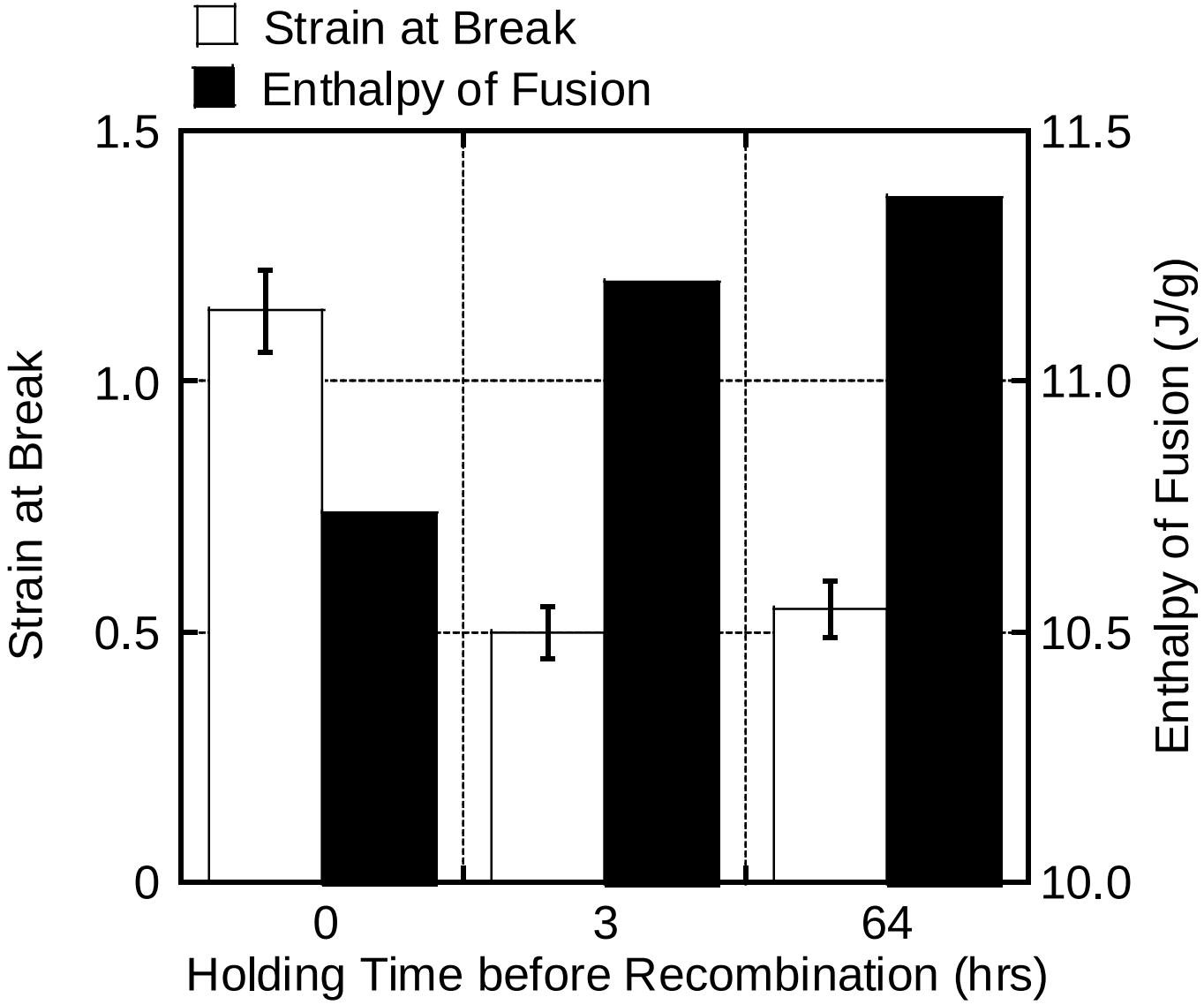

Osato et al., Figure 10

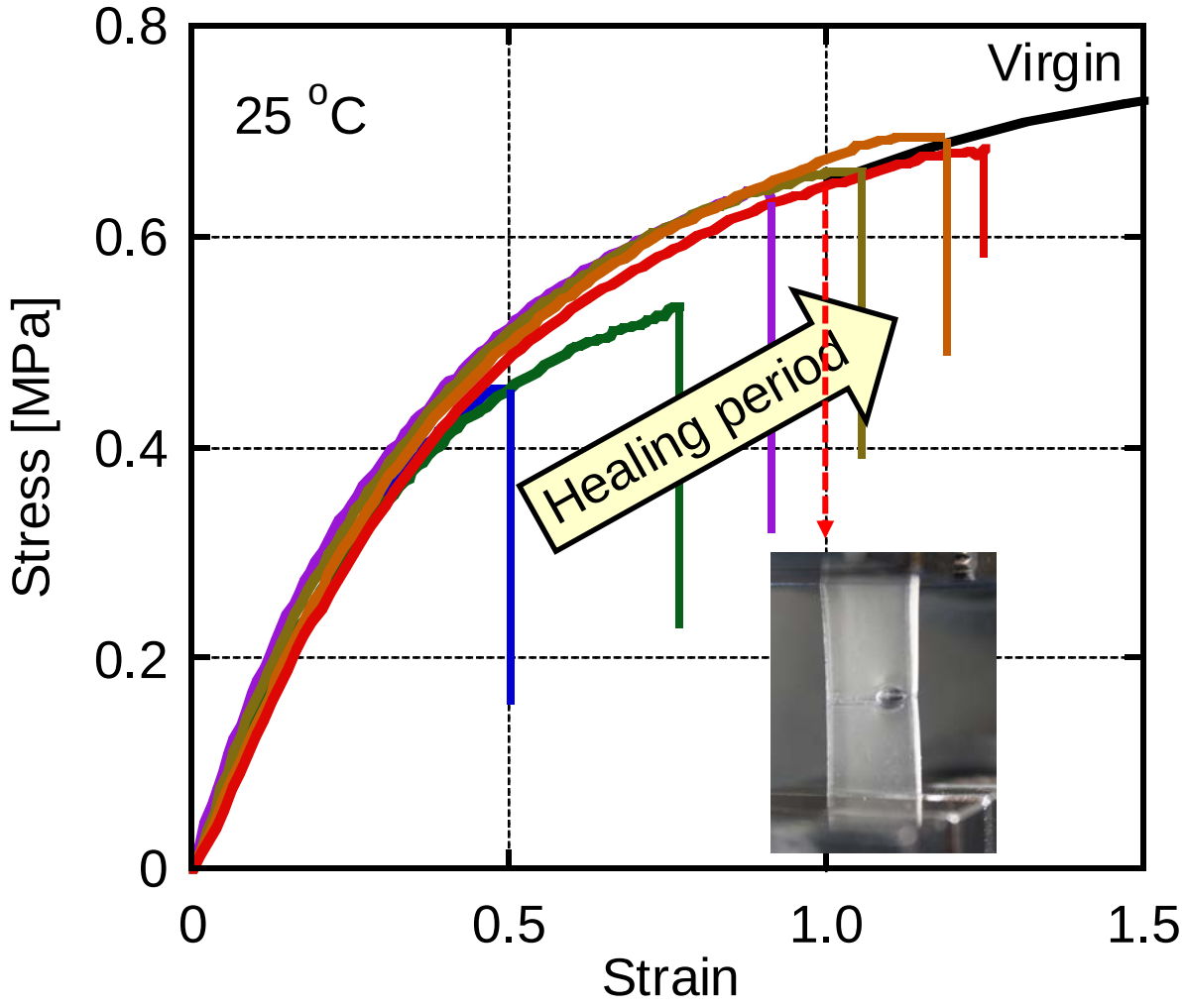
0.8
0.6
0.4
0.2
0
Stress [MPa]
25 °C
Virgin
Healing period
0
0.5
1.0
1.5
Strain